Heterogeneous catalysts—discovery and design

Graham J. Hutchings*

Received 17th July 2008, Accepted 13th October 2008
First published as an Advance Article on the web 17th November 2008
DOI: 10.1039/b812300b

Heterogeneous catalysis plays a key role in the manufacture of essential products in key areas of agriculture and pharmaceuticals, but also in the production of polymers and numerous essential materials. Our understanding of heterogeneous catalysts is advancing rapidly, especially by using the latest characterisation methods on these relatively complex effect materials. At the heart of these catalytic processes, both selective oxidation and hydrogenation play a key role. Both oxidation and hydrogenation exhibit similar requirements since often a partial reaction product is required, rather than the products of total hydrogenation or oxidation, in the latter case this being typically carbon dioxide and water. This Feature Article considers the approaches available for catalyst discovery and design for heterogeneous catalysts. Three catalysts are considered in detail, two exemplifying oxidation and the other selective hydrogenation. The design of vanadium phosphates for the selective oxidation of butane to maleic anhydride is described in terms of the search for advanced materials with superior activity. This is achieved through the synthesis of wholly amorphous vanadium phosphates. The design of supported gold and gold palladium alloy catalysts for the oxidation of carbon monoxide and the direct hydrogenation of oxygen to form hydrogen peroxide is described and the problems concerning selectivity control are discussed.

Introduction

Catalysis is one of the key underpinning technologies on which new approaches to green chemistry are based. Of the catalytic approaches available to industry heterogeneous catalysis is considered preferable in many cases. Most importantly, heterogeneous catalysis plays a major role in the general life of the general public; not only with respect to an economic viewpoint, but it also provides the necessary infrastructure for the well being of society as a whole. Without effective heterogeneous catalysis the manufacture of many materials and foodstuffs would not be possible. Redox processes such as selective hydrogenation and oxidation are two of the key synthetic steps for the activation of a broad range of substrates. They are used for the production of either finished products or intermediates. The preparation of many pharmaceuticals, agrochemicals and commodity chemicals involve selective catalytic processes. Ultimately, from a commercial viewpoint, industry prefers to use molecular hydrogen for hydrogenation reactions and molecular oxygen for oxidation, but in many cases more active forms of hydrogen, *e.g.* borohydrides, and oxygen, *e.g.* hydrogen peroxide, are used. Using H_2 and O_2 presents distinct, but different, challenges in the design of heterogeneously catalysed processes. H_2 has to be activated on the surface of a heterogeneous catalyst for it to be available for reaction under typical conditions; whereas, O_2 is a di-radical in its groundstate, and can participate in radical processes readily, even under very mild reaction conditions.

Given the widespread use of heterogeneous catalysis in many industrial processes, and the growing needs of environmental protection and green chemistry, it is interesting to consider how catalysts are discovered. Some discoveries are based on advances in materials design and synthesis. For example, the titanium silicalite TS1[1] was discovered for a range of oxidation processes using H_2O_2. In this context the design and synthesis of new zeolites[2–5] and mesoporous materials[6] have led to numerous important discoveries. Some discoveries are driven by the need to activate a specific functional group or molecule, *e.g.* Fe-ZSM-5[7] was discovered for the selective oxidation of benzene with N_2O to phenol, and supported gold catalysts[8] were discovered for the low temperature oxidation of CO. Other, more recent discoveries are based on the need to use new feedstocks, such as bio-renewable materials.[9] However, there is a key question that

School of Chemistry, Cardiff University, Cardiff, UK CF10 3AT. E-mail: hutch@cf.ac.uk; Fax: +44(0)2920874059; Tel: +44(0)2920874059

Graham Hutchings

Graham Hutchings is currently Professor of Physical Chemistry at Cardiff University and has had an interest in the discovery of heterogeneous catalysts since being introduced to the topic during his early career in industry, in ICI at Teeside, where he was introduced to vanadium phosphate catalysts. Subsequently, he was seconded by ICI to AECI, South Africa, where he made his initial discoveries concerning catalysis with gold. He moved to academia in 1984, and he has been mainly interested in the discovery and design of catalysts for oxidation and enantioselective reactions. He has held chairs in the University of Witwatersrand and the University of Liverpool before moving to Cardiff in 1997.

should be addressed. Is it possible to discover catalysts on the basis of a general approach to catalyst design? This interesting question will provide the focus for the initial part of this Feature Article, since the quest to discover catalysts for specific reactions by design remains one of the key goals in heterogeneous catalysis. After consideration of the challenges and opportunities for the discovery and design of new heterogeneous catalysts, and the key questions that need to be considered at the outset, three catalyst systems will be described in detail based on the personal experience of the author, namely:

- The selective oxidation of butane to maleic anhydride using vanadium phosphates.
- The low temperature oxidation of CO using gold supported on iron oxide.
- The selective hydrogenation of oxygen to hydrogen peroxide using supported gold and gold palladium alloys.

These three examples have been chosen as they demonstrate the complexity of heterogeneous catalysts, whilst, at the same time, demonstrating that initial solutions can be found for the design of selective catalysts. All three are examples where the interplay between materials science and catalysis could provide greatly improved catalysts.

Challenges and opportunities for catalyst discovery

With the price of energy increasing dramatically and general concerns over the availability of food, it is not surprising that these areas provide the focus for much activity in the current research on heterogeneous catalysts. For example, there is renewed interest in producing synthetic oils and fuels from CO hydrogenation using the Fischer Tropsch process, and here the key issue is can materials which give low methane together with high yields of liquid fuels be designed. On the other hand, the quest to move away from using fossil fuels to utilizing bio-renewable feedstocks as energy sources has uncovered the uncomfortable tension between the need to produce energy with a low carbon footprint whilst not endangering food supplies. At present much bio-fuels research uses materials that could be used as foodstuffs, *e.g.* maize for bio-ethanol and vegetable oils for biodiesel. However, it is clear that we need to design catalysts that are capable of deriving useable fuels from biomass that cannot be used as food, *e.g.* cellulose and ligno-cellulose.

The renewed interest in Fischer Tropsch chemistry has been generated by the requirement for low sulfur transportation fuels. As new production capacity comes on stream a range of linear alkane byproducts are becoming available that cannot be used as liquid fuels directly. Hence, there is significant interest in designing catalysts that can dehydrogenate the alkanes to alkenes, which can be used as valuable chemical intermediates in a number of processes. However, the product that is required is the terminal alkene, whereas internal alkenes are preferred thermodynamically, and isomerisation is relatively facile under the reaction conditions required for dehydrogenation. This presents a key challenge that is not yet being addressed, since virtually all research is based on using propane as a model alkane, and, of course, only the terminal alkene can be formed.

The epoxidation of alkenes is another reaction that is currently being actively researched. The epoxidation of ethene with O_2 to ethene oxide is a well established commercial process, operated globally using a promoted silver catalyst. However, the epoxidation of higher alkenes using O_2 is significantly more difficult and remains an important catalytic challenge. Epoxidation of propene using H_2O_2 with TS1,[10] or using Au/TiO_2[11] with O_2 in the presence of sacrificial H_2 are well established and give very high selectivities, but these have yet to be attained with O_2 alone.

All the reactions described above represent areas of current intense research activity in heterogeneous catalysis. However, there remain a set of grand challenges that currently are attracting less attention, although most generations in the past century have attempted to find solutions. These challenges are:

- Insertion of oxygen into a primary C–H bond to form an alcohol. There are two key targets for this; namely, the oxidation of methane to methanol and the regioselective oxidation of a linear alkane to the primary alcohol. The second of these challenges is far more demanding than the first, since, in methane, all C–H bonds are identical whereas, in longer chain alkanes, not only are there different C–H bonds, and, for many reaction strategies, the primary C–H bonds are the least reactive, but there are also C–C bonds which can readily be broken in the presence of oxidants.
- Hydrogenation of molecular oxygen to form hydrogen peroxide rather than water. Kinetically and thermodynamically this reaction represents a major challenge, since the sequential hydrogenation of hydrogen peroxide to water is favoured, and consequently any catalyst capable of the initial hydrogenation of oxygen will also catalyse this subsequent hydrogenation.
- The direct oxidation of ethane to acetic acid. This is a variation on the challenge of inserting oxygen into a primary C–H bond. However, acetic acid is particularly unstable in the presence of most oxidation catalysts at high temperatures, and typically decomposes at temperatures that are significantly lower than those required for its synthesis. At present only trace levels of selective conversion have been reported at very low conversion.
- The direct utilisation of CO_2 to form useful chemicals. Clearly this requires the input of energy and, in this case, photocatalytic processes are under active consideration. The first challenge is to find new photocatalysts that can utilise sunlight effectively. The second challenge is to identify suitable target molecules that can be synthesised. Additionally, chemical activation and utilisation of CO_2 *via*, for example, the synthesis of urea can be explored, as long as the NH_3 required for urea synthesis can be captured and recycled after the CO_2 has been transferred. Hence, there are a number of photocatalytic and chemical possibilities for CO_2 utilisation available, but finding viable strategies has, to date, eluded researchers.

In designing new catalysts for any of these grand challenges there are some key questions that should be addressed at the outset. These relate to the stability of the catalyst and the nature of the reaction mechanism. First, it is crucial to ensure that the catalyst does not degrade during use. For example, when heterogeneous catalysts are used in either gas/solid or gas/liquid/solid reactions, it is feasible that the solid catalyst can dissolve in the fluid phase. This has two consequences; first, the catalyst will clearly deactivate during use but, secondly, and more importantly, the dissolved catalytic component could act as a homogeneous catalyst. Sheldon and co-workers[12] have discussed this in detail for a number of catalysts. The effects can be subtle, and so

extreme care is required in experiments to ensure this is not occurring. In particular, sub ppm levels of some species can act as effective homogeneous catalysts and this may be difficult to observe if relatively simple experimentation involving catalyst reuse is used. Sometimes the effect is only apparent when flow reactors are used, since in stirred batch reactors, equilibria can be established between the solid and fluid phases, which mask the loss of material and the sub ppm levels of leached material are, in fact, the active catalyst species. An example of this effect is provided by TS-1 catalyst oxidation of unsaturated alcohols with hydrogen peroxide.[13] Formation of a triol by-product leads to loss of Ti^{4+} from the lattice of the titanium silicalite, but the effect only becomes significant when the catalysts are used under flow conditions when loss of Ti^{4+} becomes apparent. The leached Ti^{4+} acts as a very efficient catalyst for the formation of the triol, and so the effect is auto-catalytic.

Secondly, it is important to determine that the reaction is genuinely heterogeneously catalysed. To some extent this can be linked to the loss of species from the solid catalysts acting as homogeneous catalysts, as discussed previously. However, there is a more significant problem associated with a radical reaction mechanism that can lead to a homogeneously catalysed reaction being dominant. This is a specific problem that can be observed in oxidation reactions using molecular oxygen. As noted previously, it is not a problem that is normally encountered with hydrogenation reactions using H_2, since activation of the H_2 requires chemisorption on the catalyst surface, as the H–H bond has to be broken at some stage of the reaction. However, O_2 in its ground-state is a di-radical triplet species and so can initiate reactions that occur in the homogeneous phase, rather than being carried out heterogeneously. It is also possible that reactive radical species can be formed during the reaction on the surface of the catalyst, which are released into the fluid phase and react *via* a homogeneously catalysed reaction pathway. A key example of this behaviour is given by the work in the 1980s into the selection oxidation of methane to ethane and ethene.[14] Initially, it was considered that this was a heterogeneously catalysed process. However, it was subsequently found that the oxide catalysts, at the elevated temperature required for this reaction, all abstracted $H^{\bullet}$ from CH_4 releasing a methyl radical, $CH^{\bullet}_3$, into the gas phase. Carbon-carbon bond forming reactions are then the result of radical reactions in the gas phase.[15] Such reaction mechanisms have a profound effect both on catalyst design and, also, on the maximum yields that can be achieved. Hence, if radical reaction pathways are suspected to be involved in a reaction of interest, then it is essential that the possibility be considered that any reaction observed may not be due to heterogeneous catalysis.

Catalyst design approaches

To date, there have been relatively few generic approaches that have been proposed for the design of new heterogeneous catalysis. However, with the advent of rapid synthesis and screening technology that is inherent in recent materials science research, this is set to change. The first design approach was proposed by Dowden[16] based on a virtual reaction mechanism. Dowden used this approach to design a very effective catalyst for the oxidation of methane to methanol using O_2, one of the grand challenge reactions described earlier. In this design approach, a virtual mechanism for the reaction of interest is established, but it is important to note that the virtual mechanism may have no relationship to the real catalytic reaction mechanism. The virtual mechanism sets out the key unit steps in the overall reaction that could be components of a rate determining step. For the oxidation of methane, Dowden concluded that methane had to be dehydrogenated to achieve activation, and Fe^{3+} was known to be effective for this reaction. In addition, oxygen has to be inserted and Dowden noted that Mo^{6+} was effective for this process. Hence, he proposed that a catalyst based on a physical mixture of two oxides, Fe_2O_3 and MoO_3, would be active as a catalyst. His subsequent experiments confirmed that this was the case, and at 500 °C and at 50 bar reaction pressure the rate of methanol production was observed to be of 0.87 $kg_{methanol}/kg_{cat}h$. Indeed, this is one of the most effective catalysts identified to date for this reaction and this demonstrates the power of this approach.

We subsequently modified the virtual mechanism approach by adding a third design component.[17] For example, in the oxidation of methane to methanol, there are three crucial steps:

- The C–H bond has to be activated/broken. It was proposed that the rate of H–D exchange for the reaction of CH_4/D_2 mixture could provide a rank order of suitable oxides for the reaction. The most active oxides were found to be Ga_2O_3, ZnO and CrO_3, which, interestingly, have the same order of activity for propane aromatisation when the oxides are mixed with H-ZSM-5. As propane aromatisation requires activation of C–H bonds in an alkane, this observation provided supporting evidence for the viability of this approach.
- Oxygen has to be inserted. We proposed that the rate of $^{16}O/^{18}O$ exchange for the reaction of $^{16}O_2$ and $^{18}O_2$ mixtures over oxides could be used to obtain a rank order for oxides, and MoO_3 is the most effective oxide, but there are many other viable candidates.
- The product, in this case CH_3OH, has to be stable under the reaction conditions under which it is formed, typically elevated temperatures in the presence of excess oxygen. Many oxidations are particularly effective for the oxidation of methanol and so this is a crucial design parameter. However, it is often ignored in many catalyst design experiments.

Based on the design approach, we selected β-Ga_2O_3 as an oxide capable of activation of the C–H bond and MoO_3 for oxygen insertion. Furthermore, methanol was found to be relatively stable at elevated temperatures with both these oxides. Using a Ga_2O_3/MoO_3 physical mixture gave an enhancement in the synthesis of methanol when compared with Ga_2O_3 and MoO_3.[17] We also used this approach to select suitable supports for catalysts for ethane conversion to acetic acid.

Baerns and co-workers[18] were amongst the first researchers to use a genetic or evolutionary approach to catalyst design. At present there is significant interest in the identification of catalysts for the selective oxidative dehydrogenation of alkanes to alkenes, and the oxidation of propane is used as a model reaction, since only one alkene product is possible and this simplifies the reaction considerably. In the method proposed by Baerns and co-workers[18] they selected eight oxides known to be active for alkane oxidation. These oxides need not necessarily be catalysts for selective oxidation, rather they just need to show some alkane oxidation activity. They selected the oxides of V,

Mg, B, Mo, La, Mn, Fe and Ga. They then selected different groups of four of these oxides and prepared mixed oxides. From this first generation the best were identified using catalyst testing for propene oxidation. These were then used as the basis for the second generation, in which one of the four oxides was replaced by another from the list of eight oxides. This iterative process was then continued through subsequent generations. The best catalyst identified was $V_{0.22}Mg_{0.47}Mo_{0.11}Ga_{0.2}O_x$ which gave a yield of 9% propene.[18] However, it should be noted that the material identified is related to $VMgO_x$ which was one of the first catalysts to be identified for this reaction. It would, therefore, be interesting to determine the outcome of this approach if both V_2O_5 and MgO were omitted from the group of eight selected oxides at the start. There are two key advantages of this approach. First, it decreases the number of experiments that are required in identifying potential selective catalysts; for example, in the example described only 600–1000 experiments were conducted, but 20 900 would have been required if the full set of permutations was evaluated. Secondly, the composition of the materials being investigated does not need to be known in detail. Only materials exhibiting sufficient activity need to be characterized. Hence, the evolutionary approach can play a valuable role in the future of catalysts design when coupled with high throughput preparation and testing. However, all three approaches described have merit in designing catalysts. The key point is that once a suitable initial formulation is identified, then detailed preparation of a number of target materials can be initiated.

Designing vanadium phosphate catalysts for the selective oxidation of butane

Vanadium phosphates have been used as catalysts for the selective conversion of butane since their discovery in 1966.[19] They are used extensively for the commercial production of maleic anhydride and typically butane, below the lower explosive limit, is reacted with air at temperatures in the range of 350–480 °C. The reaction represents a very deep oxidation with the removal of four hydrogen atoms as water and the insertion of three oxygen atoms, and yet selectivities to maleic anhydride up to 80% can be achieved. This is because maleic anhydride is kinetically stable to subsequent oxidation over vanadium phosphates under these conditions. This is a key factor as was highlighted previously, *i.e.* the product should be stable under the reaction conditions used. In addition, the oxidation of butane using vanadium phosphates involves lattice oxygen and there are no complications from gas phase oxidation even though elevated temperatures are used.

Since their initial discovery as catalysts for butane oxidation, vanadium phosphates have been extensively studied.[20–24] In general, most studies have utilized catalysts prepared from a hemihydrate precursor, $VOHPO_4 \cdot 0.5H_2O$, which is transformed by heating in the reaction mixture, primarily to the pyrophosphate, $(VO)_2P_2O_7$, as well as a complex mixture of minor components comprising $VOPO_4$ phases as well as amorphous material.[25] Given the complexity of this catalyst, the question arises as to which of the phases present are active.

There are many ways of preparing $VOHPO_4 \cdot 0.5H_2O$, and three typical methods,[25] designated VPA, VPO and VPD are shown in Scheme 1

VPA Route

$$V_2O_5 + HCl \xrightarrow[2.\ H_3PO_4]{1.\ \Delta,\ 2h} VOHPO_4.\tfrac{1}{2}H_2O$$

VPO Route

$$V_2O_5 + H_3PO_4 + \text{alcohol} \xrightarrow{\Delta,\ 16h} VOHPO_4.\tfrac{1}{2}H_2O$$

VPD Route

$$V_2O_5 + H_3PO_4 \xrightarrow[\Delta,\ 16h]{H_2O} VOPO_4.2H_2O \xrightarrow[\Delta,\ 16h]{\text{alcohol}} VOHPO_4.\tfrac{1}{2}H_2O$$

Scheme 1

All three methods produce $VOHPO_4 \cdot 0.5H_2O$, as determined by powder X-ray diffraction (Fig. 1–3), but with different morphologies. The material prepared using aqueous HCl as the reducing agent for V_2O_5 tends to give larger crystallites (Fig. 1) compared with the VPO (Fig. 2) and the VPD material comprises rosettes of very thin platelets (Fig. 3). Following activation in butane the three hemihydrates give very different materials (Fig. 4), although they have been exposed to identical reaction conditions.[25] Characterisation by scanning electron microscopy shows that the three materials retain the morphology of the initial hemihydrate, which is expected as the transformation to the activated material is known to be topotactic.[26] However, the X-ray powder diffraction patterns and the ^{31}P nmr spin echo mapping spectra clearly show key differences. ^{31}P spin echo mapping nmr spectroscopy is a powerful technique for the determination of the environment of the vanadium in vanadium phosphates, and typically $VOPO_4$ phases give a sharp resonance at $\delta = 0$ ppm, $(VO)_2P_2O_7$ gives a broad resonance at $\delta = 2400$ ppm and disordered V^{4+}-V^{5+} dimers give a broad signal at $\delta =$ 1100 ppm. The material derived from VPA-hemihydrate comprises mainly V(V) $VOPO_4$ phases, the activated VPO-hemihydrate shows very little structure in the X-ray diffraction pattern, but by ^{31}P spin echo mapping nmr spectroscopy the material comprises mainly $VOPO_4$ phases with some disordered

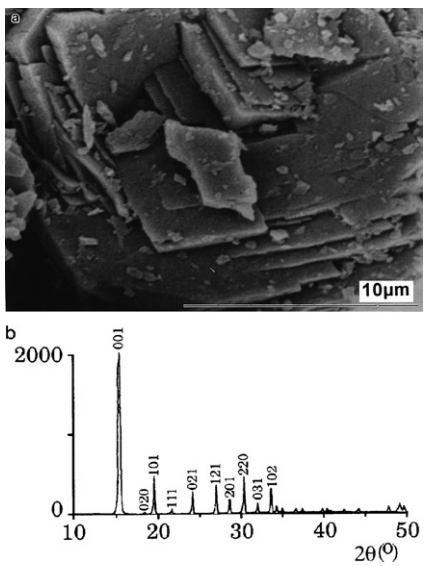

Fig. 1 SEM and XRD characterization of $VOHPO_4 \cdot 0.5H_2O$ prepared by the VPA route.[25]

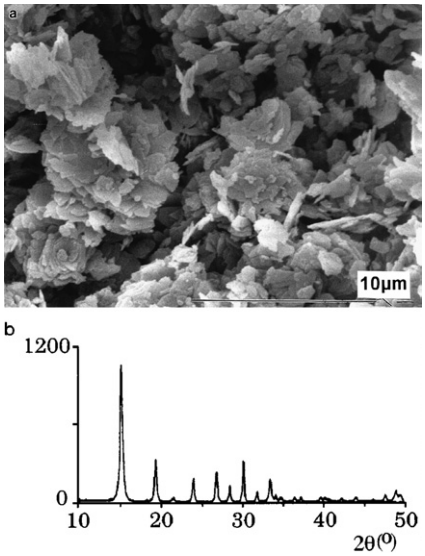

Fig. 2 SEM and XRD characterization of $VOHPO_4 \cdot 0.5H_2O$ prepared by the VPO route.[25]

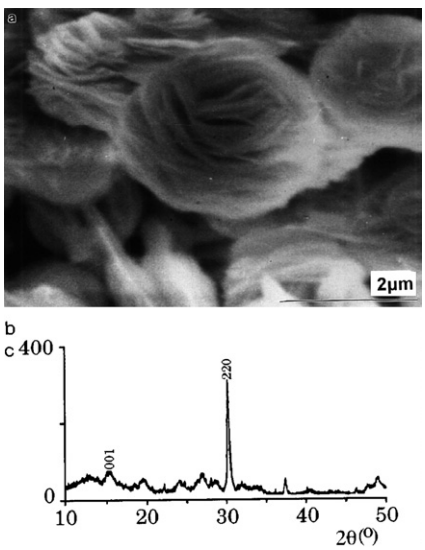

Fig. 3 SEM and XRD characterization of $VOHPO_4 \cdot 0.5H_2O$ prepared by the VPD route.[25]

V^{4+}-V^{5+} material and a smaller amount of $(VO)_2P_2O_7$. However, the activated material derived from the VPD-hemihydrate comprises mainly $(VO)_2P_2O_7$ with smaller amounts of disordered V^{4+}-V^{5+} material and $VOPO_4$ phases. Given the differences in the catalyst compositions it could be expected that these materials would show very different activities. However, this was not observed and the surface area-corrected rates of butane conversion are identical.[24] Indeed, attempts to make the hemihydrate by different methods[21] (*e.g.* using V_2O_4 in place of V_2O_5, or using H_3PO_3 as a reducing agent) all lead to activated materials with very similar activity per unit surface area, although the phase composition and morphologies of the materials are all very different.[27] The methods for preparing the hemihydrate, described so far, all involve reactions at ambient pressure. The effect of increasing the temperature and using higher pressures by using an autoclave for the preparation has been studied for the reaction of $VOPO_4 \cdot 2H_2O$ with octan-1-ol.[28] Three distinct materials can be formed depending on the conditions (Fig. 5). At low temperatures and atmospheric pressure, the $VOPO_4 \cdot 2H_2O$ is exfoliated with the alcohol being occluded within the structure.[29,30] Up to 200 °C the hemihydrate phase is formed, and at higher temperatures and pressure the tetragonal form of $VPO \cdot H_2O$ is formed. However, on activation and testing all these materials give similar activity per unit surface area for butane activation.[28]

The realization that the catalyst activity for butane oxidation to maleic anhydride is dependent solely on the exposed surface area of the activated catalysts has, to some extent, arrested progress in this field, since methods that give sufficient exposed surface area for use in the commercial process are already well known. However, given the wide range of materials that comprise these active catalysts the observation of a single specific activity is intriguing, and prompted us to investigate the origin of this effect, and, in particular, the possible role played by amorphous vanadium phosphate material, since these disordered materials are often found to be present in active catalysts. Detailed investigation of the surface of vanadium phosphate crystallites using high resolution transmission electron microscopy has shown that the surface has an amorphous overlayer (Fig. 6).[24,27] This observation would explain why the catalysts all have a similar activity per unit surface area, as the materials could all have a similar amorphous surface overlayer that is stabilized on heating in a butane air atmosphere at 400 °C. Of course, the evidence concerning the observation of a surface amorphous overlayer has to be viewed with care since this may result from a combination of one or more of the following processes: (i) exposure of the crystalline surfaces to the reactor feed producing amorphous material *in situ*, (ii) electron beam damage of the $(VO)_2P_2O_7$ crystallites (which are known to completely amorphise after 20–30 s under typical electron beam irradiation conditions in the microscope) and/or (iii) preferential electron beam sensitivity of a crystalline surface layer (*e.g.* $VOPO_4$ which is known to completely amorphise in a few seconds in the electron beam of the microscopy). Hence, it is not possible, with transmission electron microscopy alone, to determine unequivocally whether the presence of a surface amorphous layer is simply an artefact due to beam damage or is, indeed, the genuine catalytically active phase.

However, a number of studies have indicated that disordered materials can play an important role.[31–52] Additional evidence in support of the proposal that the surface layer of the crystallites of vanadium phosphate is significantly different from the bulk is provided by the following observations: (a) X-ray photoelectron spectroscopy consistently shows phosphorus enrichment in the surface layers ($P : V \geq 1.5$) indicating that the surface is significantly different from the bulk structure of the crystallites.[20,52] Fully crystalline structures of $(VO)_2P_2O_7$ and $VOPO_4$ would not be able to provide this degree of phosphorus enrichment. Furthermore, the phosphorus enrichment is enhanced during the transformation of the precursor $VOHPO_4 \cdot 0.5H_2O$ to the final catalyst. (b) Catalyst activity can be enhanced by the addition of promoters,[52,53] in particular Co is found to be particularly effective. For the vanadium phosphate catalyst prepared using

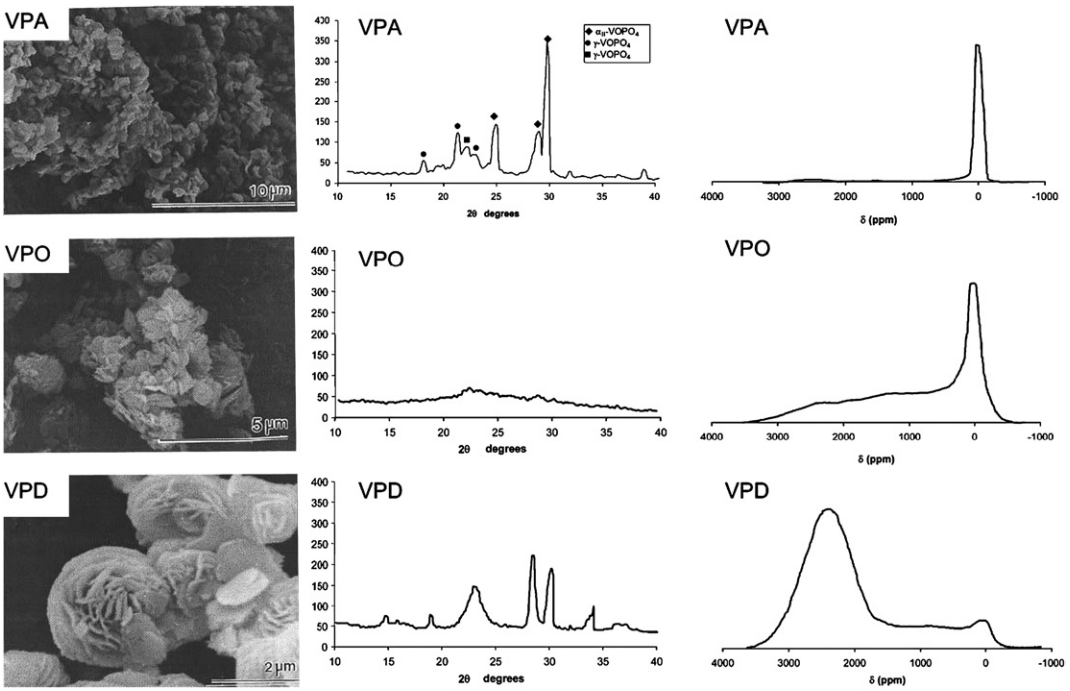

Fig. 4 SEM and XRD and ^{31}P spin echo mapping characterization of activated catalysts produced from the $VOHPO_4 \cdot 0.5H_2O$ prepared by the VPA, VPO and VPD routes.[25]

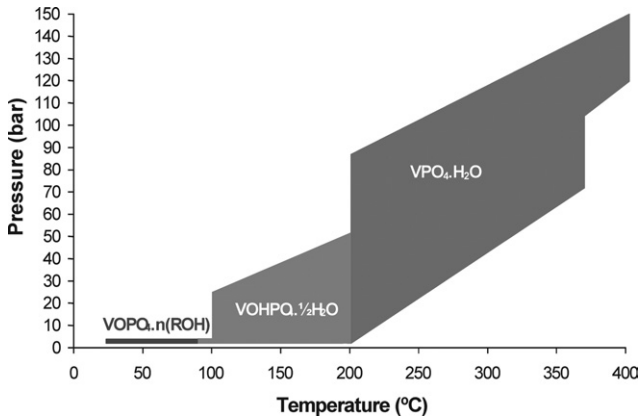

Fig. 5 Effect of temperature and pressure on the products that can be formed in the reaction of $VOPO_4 \cdot 2H_2O$ and 1-octanol.[28]

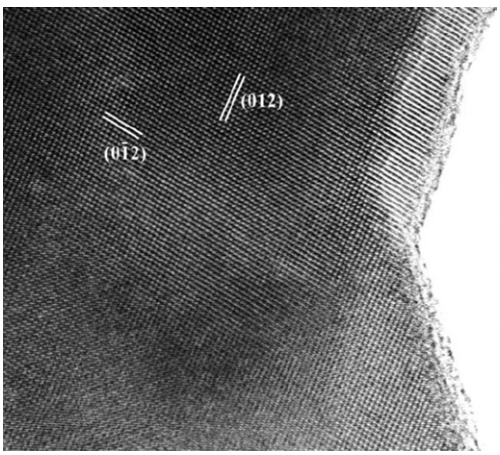

Fig. 6 HRTEM image of an activated vanadium phosphate catalyst. The bulk material is crystalline $(VO)_2P_2O_7$ and the surface has an amorphous overlayer.[24]

the VPO route the Co was found to preferentially be associated with the amorphous material, and appeared to stabilize the retention of amorphous material in the activated catalyst.[54] Co was not found to be present (to the analytical detection limit) in the crystalline $(VO)_2P_2O_7$, yet the intrinsic activity of the Co-containing catalyst was enhanced by a factor of 3. This indicates that Co promotes the catalytic performance of the amorphous material derived from this preparation method. (c) Oxidation of $(VO)_2P_2O_7$ has been shown to enhance the selectivity to maleic anhydride and oxidise the surface of the catalyst.[43] This oxidation treatment also correlates with an increase in the depth of the amorphous overlayer as observed on edge-on the $(VO)_2P_2O_7$ crystallites viewed using very low illumination transmission electron microscopy.

These observations are also supported by the discovery that a wholly amorphous vanadium phosphate can be prepared using supercritical CO_2 ($scCO_2$) as an antisolvent.[31,55] The use of $scCO_2$ as an anti-solvent for the controlled precipitation of materials from conventional solvents has been widely applied to the production of a range of materials. These include polymers, pharmaceutical chemicals, explosives, superconductors, and catalysts.[56–59] When a solution is brought into contact with $scCO_2$, the solvent power of the conventional solvent is reduced, and the solutes precipitate. Hence $scCO_2$ can play the role traditionally taken by the base, *e.g.* sodium carbonate, in conventional co-precipitation. In this case the base can be

substituted in a conventional co-precipitation by using $scCO_2$, and we have used this to prepare a very active form of CeO_2 as a catalyst support.[60] The diffusivity of $scCO_2$ is about two orders of magnitude higher than that of conventional liquids. This rapid diffusion can produce supersaturation immediately before precipitation, leading to the formation of nanoparticle morphologies not usually accessible by standard catalyst preparation methods. Hence, this new method provides access to materials that cannot readily be prepared by conventional precipitation routes. We have explored using $scCO_2$ for vanadium phosphate synthesis,[31,55] and we had to modify the preparation procedure since the starting point is a solution containing vanadium and phosphorus in a solvent that $scCO_2$ can diffuse into and act as an antisolvent. To achieve this a solution of H_3PO_4 in isopropanol was refluxed with $VOCl_3$ for 16 h and the solution was processed using $scCO_2$, to precipitate a vanadium phosphate.[31,55] We also prepared a vanadium phosphate by evaporation of the solution by refluxing $VOCl_3$ and H_3PO_4 in isopropanol. This non-$scCO_2$ material, as expected, exhibited the same specific activity as the VPO and VPD materials described earlier. However, the sc-VPO material exhibited a much higher specific activity (Fig. 7). Interestingly, and in total contrast to vanadium phosphates prepared using the VPO and VPD methods,[25] the sc-VPO material did not require any reaction time to become active,[31] whereas the VPO and VPD typically require several hours under reaction conditions before they reach their optimal activity.[25,31] Examination of the $scCO_2$-VPO material by electron microscopy showed that both the fresh and used catalysts comprised spheroidal particles (Fig. 8) that are not changed on exposure to the reaction gases. Furthermore, selected area electron diffraction analysis of both the precursor and activated catalysts derived from the sc CO_2-VPO showed that they were amorphous. This is consistent with the fact that the particles show no crystallographic faceting and adopt a minimum surface area (*i.e.*, spherical) morphology. Interestingly, this method of preparation is very sensitive to the solvent that is used since changing the alcohol from isopropanol to isobutanol results in a material that comprises some crystalline material (Fig. 8) and this is a much less effective catalyst.[25]

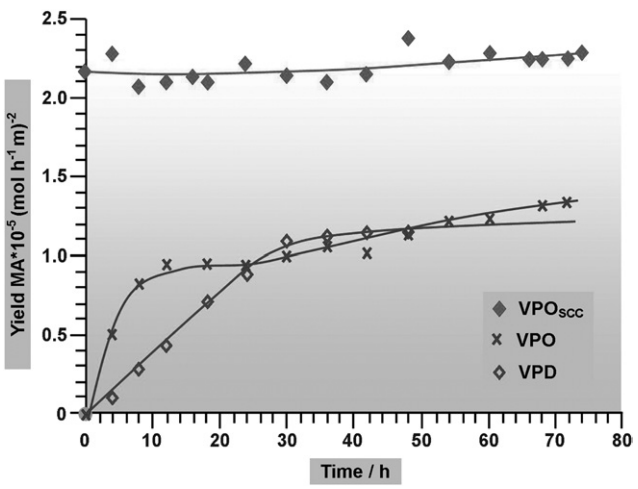

Fig. 7 The activity of vanadium phosphate catalyst at 400 °C, contrasting the activity of the amorphous material with the standard catalysts.[31]

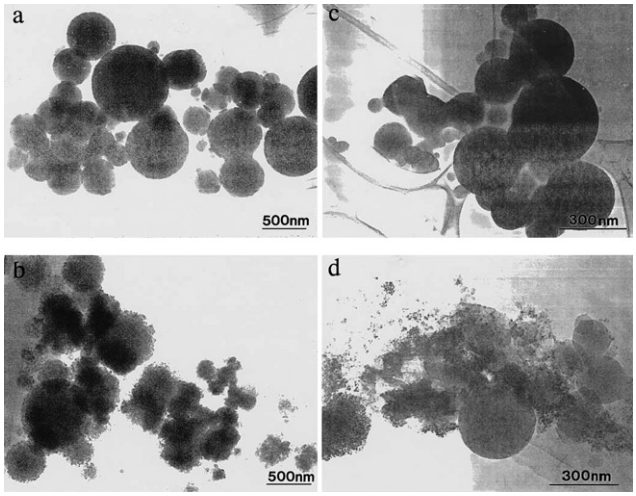

Fig. 8 Transmission electron micrographs of (a) material prepared using isopropanol prior to catalyst testing, (b) material prepared using isopropanol after catalyst testing, (c) material prepared using isobutanol prior to catalyst testing, (d) material prepared using isobutanol after catalyst testing.[31]

The use of $scCO_2$ as an antisolvent in the preparation of vanadium phosphates opened up the possibility of preparing a new amorphous material, which was much more active than the conventional vanadium phosphates. However, detailed analysis of the sc-VPO using XPS, NEXAFS and ^{31}P spin echo mapping nmr spectroscopy showed that sc CO_2-VPO material was very different from the catalysts derived from the conventionally derived hemihydrate precursor.[31] Hence, this material may not be related to the amorphous material that is observed as an overlayer in the transmission electron microscopy analysis of vanadium phosphorus catalysts derived from $VOHPO_4 \cdot 0.5H_2O$.[24,27] The possibility that the amorphous overlayer could originate from an unstable $VOPO_4$ phase, as discussed previously in this article, prompted us to study ω-$VOPO_4$ in detail,[61] since this phase is metastable and is thermally unstable below 350 °C, which, of course, means that this material is stable in the temperature range used for butane oxidation, *i.e.* 350–480 °C. We initially showed that ω-$VOPO_4$ could be formed by heating $(VO)_2P_2O_7$ in O_2 at 625 °C, and that it could be formed and decomposed reversibly by cycling the temperature between 25 and 400 °C in O_2.[61] We also showed that ω-$VOPO_4$ had similar activity for butane oxidation to the VPO and VPD materials as described previously. The sensitivity of the long-range ordering of ω-$VOPO_4$ was studied at 400 °C using a number of chemical environments that would be expected to be present during butane oxidation. In addition, we used three complementary *in situ* techniques, namely powder X-ray diffraction, EPR spectroscopy and laser Raman spectroscopy to study the complex interplay between vanadium phosphates under reaction conditions. Initially, we tested the stability of ω-$VOPO_4$ in air, with and without added water vapor, since water is formed in the selective oxidation of *n*-butane to maleic anhydride. In both cases, ω-$VOPO_4$ was stable at 400 °C and no hydration was observed. Next, we exposed ω-$VOPO_4$ to four different *n*-butane environments: 1.5(Fig. 9), 3 and 5% *n*-butane in air, and 5% *n*-butane in N_2 (Fig. 9). The ω-$VOPO_4$ was always

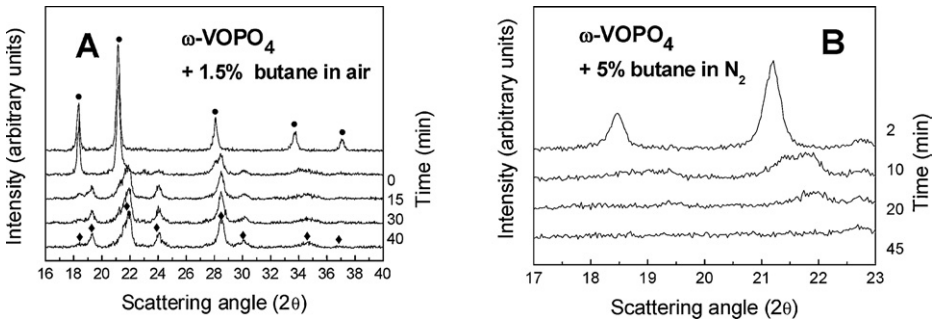

Fig. 9 *In situ* XRD pattern of w-$VOPO_4$ (●) after treatment at 400 °C with butane specified. Depending on the reactant, ω-$VOPO_4$ may transform quickly to δ-VOPO4 (◆) (A), or transform quickly into d-$VOPO_4$ and subsequently into a disordered phase (B).[61]

stabilised in the *in situ* diffraction cell in air or N_2 at 400 °C before adding the *n*-butane at the specified concentration. With 1.5% butane in air, ω-$VOPO_4$ transformed rapidly to δ-$VOPO_4$. The crucial observation is that the transformation is very rapid, and was complete within minutes. Since powder X-ray diffraction examines the bulk structure, these experiments suggest a close structural correlation between ω-$VOPO_4$ and δ-$VOPO_4$ and this was confirmed.[61] When the amount of butane was increased, the same effects were observed, and a rapid transformation to δ-$VOPO_4$ occurred. However, if the reaction was carried out in the absence of air, ω-$VOPO_4$ initially transformed into δ-$VOPO_4$ and then rapidly converted into a largely disordered material (Fig. 9). This transformation was accompanied by a chemical reduction, as confirmed by X-ray photoelectron and EPR spectroscopy. We proposed that the initial trigger for the structural changes observed was the removal of surface lattice oxygen, which was replaced from the bulk structure by diffusion and this leads to a disordered material being formed. Similar fast transformations of ω-$VOPO_4$ to δ-$VOPO_4$ were observed with acetic acid/air reaction gases, and slower transformations with CO and H_2 both of which can be considered to be more potent reducing agents than alkanes for many materials. Interestingly, no reaction was observed with maleic anhydride/air mixtures, which is probably related to the stability of this product over vanadium phosphates at these temperatures. Also, δ-$VOPO_4$ and the disordered material could be transformed back to ω-$VOPO_4$ on heating in air at 600 °C. The summary of the findings (Fig. 10) shows the complexity of the interplay that is possible with these vanadium phosphate phases. In view of these findings, it is clear that the vanadium phosphate catalyst system is very complex when studied under reaction conditions, and that disordered materials may be formed in a transitory manner and yet these may be the crucial phases responsible for catalyst activity. However, this study also demonstrates the crucial importance of *in situ* investigations of active catalysts if we are to discover the nature of the active phases, and hence ensure improved catalysts can be designed.

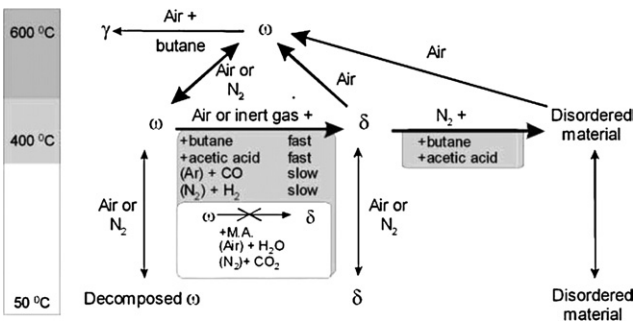

Fig. 10 Summary of ω-$VOPO_4$ transformations observed between 50– and 600 °C. ω-$VOPO_4$ transforms to δ-$VOPO_4$ when exposed to a variety of reactants at 400 °C. A further transformation of δ-$VOPO_4$ into a disordered material was observed when butane or acetic acid was added in the absence of oxygen. δ-$VOPO_4$ recrystallized to ω-VOPO4 when calcined at 600 °C in air. The disordered material obtained in the butane experiment recrystallized to ω-$VOPO_4$ when calcined at 600 °C in air. ω-$VOPO_4$ transforms irreversibly to γ-$VOPO_4$ when exposed to butane in air at 600 °C.[61]

Designing supported gold and gold palladium catalysts

It is well known today that gold when prepared on the nanoscale is very effective as a redox catalyst.[62–73] The dramatic increase in interest in using gold catalysts springs from two discoveries made contemporaneously in the 1980s by Haruta and Hutchings[8,74,75] who demonstrated that gold could be not just an outstanding catalyst but could be the best catalyst for a reaction, namely low temperature CO oxidation catalysed by gold nanoparticles[8] and acetylene hydrochlorination catalysed by cationic gold.[75] Haruta made the unexpected discovery that gold, when divided to the nanoscale, to just a few hundreds of atoms, can be the most effective catalyst for the oxidation of CO at temperatures as low as −76 °C.[8,76] This key discovery by Haruta that gold nanoparticles could act as effective oxidation catalysts has led to an explosion of interest in gold catalysis. The extensive work in this field has been extensively reviewed,[62–73] In particular, the extensive literature on the CO oxidation reaction using gold catalysts has recently been discussed in detail.[77] However, in relation to catalyst discovery, the supported gold nanoparticles demonstrate a useful example. Active catalysts are typically prepared by a coprecipitation process. For example for TiO_2-supported catalysts, deposition precipitation is used where the TiO_2 is stirred in an aqueous solution of a gold salt and base is added to precipitate the gold,[78–82] whereas Fe_2O_3-supported catalysts are prepared by coprecipitation from an aqueous solution of gold and iron salts.[83–85] These methods tend to synthesize a very broad range of gold nano-structures and until recently particles in the 2–5 nm range were considered to be the active species in these catalysts.[85] However, transmission electron microscopy has advanced rapidly, especially with the introduction of

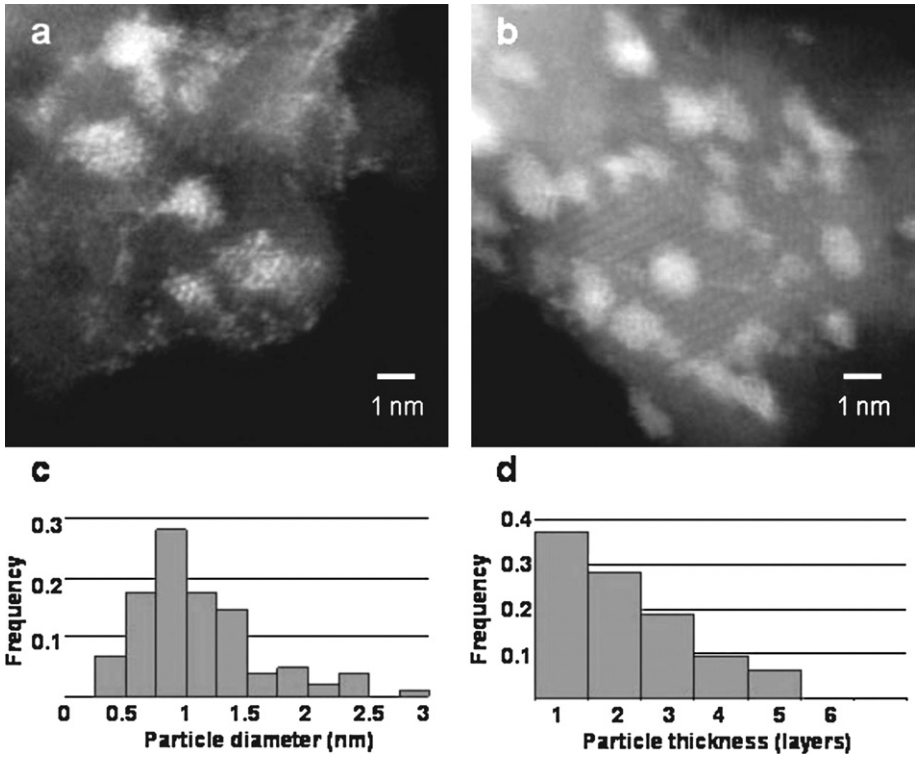

Fig. 11 High-magnification *Z*-contrast micrographs showing 10 wt % loaded Au on anatase, obtained by Pennycook and co-workers,[86] after two stages of preparation. (a) In the oxidized precursor state following deposition-precipitation of Au, many individual Au atoms are sharply resolved. (b) In the most active form, after mild reduction in 12% H_2 at 150 °C, individual neutral Au atoms are not resolved. (c) Histogram of the distribution of 103 Au particle diameters in the reduced sample. Single atoms and particles over 10 nm were not included. Mean particle size was 1.1 ± 0.5 nm. (d) Histogram of the approximate distribution of 32 selected Au-particle thicknesses in the reduced sample determined from relative intensities of *Z*-contrast images.

aberration-corrected scanning transmission electron microscopy (STEM), which has enabled much smaller structures to be observed. Recent cutting edge research[86] has shown the range of structures present from a typical preparation (Fig. 11). The method produces a very broad distribution of gold nanoparticles from sub-nanometre, *i.e.* just a few atoms, to particles >2 nm. Previously, until the advent of this technique only the larger structures were observed, and hence the activity was attributed to their presence. We now know that much smaller structures are present in the catalysts that are active for low temperature CO oxidation. However, the fact that the preparation method produces a broad range of structures is of great value in the catalyst discovery phase, since we do not know which structures are active, and so we have the greatest chance of having at least some of the active structures present. Of course this means that most of the gold present in these catalysts is, perhaps, inactive, and hence the second phase of catalyst design concerns the identification of the active structures and their target synthesis. It is clear that in the field of gold catalysis we are only just entering phase 2 as we seek to understand the nature of the active site.

Recently, we have used aberration-corrected STEM to unravel which structures in a supported gold catalyst are associated with high activity for Au supported on FeOOH, which is known to be a very active catalyst for CO oxidation. We have previously studied this catalyst in great detail[87] and in the course of this investigation we reported some intriguing results concerning the link between catalyst performance and catalyst drying conditions. We had synthesized a pair of 2.9 at% Au/FeO_x samples (denoted A, B) were derived from the same co-precipitated precursor. Sample A, was dried in a tube furnace in static air, while B was dried in flowing air, both at 120 °C for 16 h. The Au loading in each was identical and the underlying support was disordered FeOOH with similar surface areas (*ca.* 190 m^2g^{-1}). X-Ray energy dispersive spectroscopy (XEDS) analysis and high-angle annular dark-field (HAADF) imaging experiments indicated that both samples contained 2–15 nm Au particles, with mean particle sizes of 5.4 nm for A and 7.0 nm for B (Fig. 12). If particle size was the key factor governing the activity

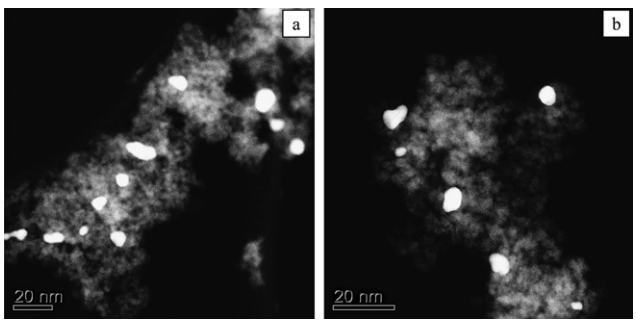

Fig. 12 Low magnification aberration-corrected HAADF-STEM images from (a) the inactive, tube furnace catalyst (sample A) and (b) the highly active, GC oven catalyst (sample B). Au particle size distribution in both samples appears to be very similar at this magnification.[86]

of supported gold catalysts then these two samples should have similar activity. However, catalytic testing of the samples using standard conditions (total flow rate 66 000 vol gas/vol catalyst h, 0.5 vol% CO), revealed that B achieved 100% CO conversion at 25 °C, whereas A gave only trace CO conversion (*i.e.* <1%). In our initial study[87] we were unable to determine the origin of this striking effect due to resolution and sensitivity limitations of the characterization techniques available. We have now re-examined these samples using a state-of-the-art aberration-corrected STEM.[88] Using this higher magnification, (Fig. 13) it is possible to determine that the Au particle size distribution and morphology in these samples is quite different. Both samples do indeed contain similar numbers of larger (2–15 nm) Au particles (Fig. 12). However, it is now possible to image individual gold atoms. Both samples contain a significant number of individual Au atoms (Fig 13, indicated by red circles) dispersed on the iron oxide surface. However, the active sample B also contained a large number of sub-nanometre Au clusters (Fig 13, circled in yellow), which were absent in the inactive sample A. These Au clusters, the majority of which were 0.2–0.5 nm in diameter, contain at most only a few Au atoms, but this study shows clearly that it is these very small species that are active in gold catalysis for CO oxidation. In a subsequent part of this study[81] we demonstrated that it is the bi-layer nanoclusters containing around 10 atoms, rather than the smaller monolayer structures, that are the active species. This study provides a valuable link with model catalyst studies which have previously demonstrated that extended bi-layer Au structures supported on a titanium dioxide substrate are exceptionally active for low temperature CO oxidation.[89] The challenge now facing materials scientists is how to synthesize and stabilize these structures in high concentrations, since there population based on the total number of gold atoms present in real catalysts is very small.

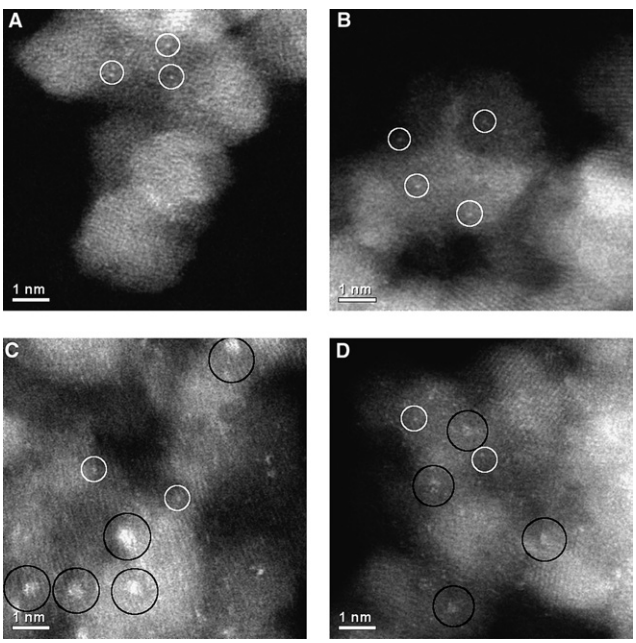

Fig. 13 High-magnification aberration-corrected STEM-HAADF images of the inactive (A) (a and b) and active (B) (c and d) Au/FeO_x catalysts acquired with the aberration-corrected JEOL 2200FS. The white circles indicate the presence of individual Au atoms while the black circles indicate sub-nm Au clusters consisting of only a few atoms (yellow circles). Note the presence and image intensity difference of two distinct cluster-types: in (c) there are 0.5 nm, higher contrast clusters whereas in (d) 0.2–0.3 nm low-contrast clusters dominate. This indicates the presence of bi-layer and monolayer sub-nm Au clusters in the active catalyst.[87]

Highly dispersed supported gold nanoparticles have been found to be active for a range of reactions,[68] including the preferential oxidation of CO in the presence of H_2, CO_2, and H_2O for fuel cell applications,[84,85] the oxidation of alcohols,[90] the epoxidation of alkenes[91–95] as well as the hydrogenation of unsaturated aldehydes,[96] the hydrogenation of alkynes in the presence of alkenes,[97] the hydrosilylation of alcohols and aldehydes[98] and the hydrogenation of N–O bonds.[99] Supported gold catalysts are therefore very versatile and in many of these applications they give the best catalyst performance observed to date. Au/Al_2O_3 catalysts were also observed to display activity in the direct formation of hydrogen peroxide by the reaction of H_2 and O_2 at low temperature.[100–108] However, this catalyst gave low selectivity based on H_2 utilisation and was much poorer in terms of catalyst performance when compared with supported Pd catalysts which had, up to that date, been studied for this reaction. Indeed, studies concerning the direct formation of hydrogen peroxide using Pd catalysts date back for almost a century. However, the combination of Au and Pd in supported alloys gave a synergistic enhancement in the activity and selectivity for both Au and Pd,[100–108] and this has now been demonstrated on many supports (Table 1).[105] Carbon and silica supports give the best performance as judged in terms of the yield of hydrogen peroxide that is achieved under these conditions. The synergistic effect is most pronounced for carbon-supported catalysts since in the absence of Pd these catalysts demonstrate very limited activity, but the combination of Pd and Au gives a marked enhancement over both the Au- and Pd- only catalysts. We subsequently showed that the catalysts were also highly active for alcohol oxidation using solvent-free conditions.[109]

Table 1 The formation of hydrogen peroxide using Au, Pd and Au–Pd supported catalysts[a],[105]

Catalyst	Hydrogen peroxide formation (mol H_2O_2/kg_{cat} h)	Hydrogen selectivity (%)
5% Au/silica	1	nd
2.5% Au–2.5% Pd/silica	108	80
5% Pd/silica	80	80
5% Au/Carbon	1	nd
2.5% Au–2.5% Pd/Carbon	110	80
5% Pd/Carbon	55	34
5% Au/Al_2O_3	2.6	nd
2.5% Au–2.5% Pd/Al_2O_3	15	14
5% Pd/Al_2O_3	9	nd
5% Au/TiO_2	7	nd
2.5% Au–2.5% Pd/TiO_2	64	70
5% Pd/TiO_2	30	21

[a] Reactions were carried out in a stainless steel autoclave with the catalyst (0.01 g), solvent (5.6 g MeOH and 2.9 g H_2O), and a mixture of 5% H_2/CO_2 and 25% O_2/CO_2 to give a hydrogen to oxygen ratio of 1: 2 at a total pressure of 3.7 MPa. Stirring (1200 rpm) was commenced on reaching the desired temperature (2 °C), and the reaction was carried out for 30 min; nd = not determined as the yield is too low for reliable measurement.

The key problem that dominates the catalytic formation of hydrogen peroxide using the direct reaction is the selectivity of H_2 utilisation. This is a crucial factor since the direct process has to demonstrate almost total selectivity for H_2 usage if it is to compete with the commercially well established indirect process[107,108,110] which achieves *ca.* 95% selectivity. The current indirect process for hydrogen peroxide involves the sequential hydrogenation and oxidation of an alkyl anthraquinone, thereby avoiding the use of potentially explosive mixtures of hydrogen and oxygen.[110] However, the process has a number of disadvantages, and consequently a direct process could be preferred if the selectivity issue can be addressed. This is therefore the key aspect that should be addressed in the design of these Au–Pd catalysts. The primary reaction is the hydrogenation of di-oxygen, and hence the H_2 has to be activated. Consequently any catalyst that is active for the initial hydrogenation reaction will almost certainly be active for the secondary hydrogenation of hydrogen peroxide to water. In addition, there are two other pathways by which non-selective chemistry can occur and the full range of reactions is shown in Scheme 2.

This problem has been well known for the direct synthesis of hydrogen peroxide for decades, and, indeed, it is at the heart of many catalytic reactions where a reactive intermediate is the required product but its subsequent reactions are often kinetically favoured over its synthesis. In the case of supported Pd catalysts, promoters such as halides (Br^-) and phosphoric acid are added to stabilise the hydrogen peroxide, by ensuring that the rate constants for hydrogen peroxide consumption (k_2 and k_4) are decreased relative to the rate constant for synthesis (k_1).[111–114] Indeed, these promoters are essential when using supported Pd catalysts, and some of the highest productivity data has been disclosed by researchers from Solvay Interox, notably Van Weynbergh *et al.*,[114] using supported Pd catalysts with N_2 as diluent. Interestingly, we have shown[107] that the addition of Br^- and H_3PO_4 to the reaction mixtures for the high activity supported Au–Pd catalyst is deleterious (Table 2), whereas these promoters have to be present for the monometallic supported Pd catalysts. As the Au–Pd catalysts do not leach gold or palladium into solution we concluded that the loss in activity could be due to the anions blocking sites on the catalyst surface that are active for the synthesis of hydrogen peroxide. Indeed, it is a most significant observation that the supported Au–Pd catalysts do not require the addition of Br^- and phosphate promoters and readily produce hydrogen peroxide yields that are comparable to, or even higher than, those of the Pd catalysts under the optimal conditions using the added promoters. This finding clearly demonstrates key differences must exist in the structures of the monometallic Pd catalysts and the Au–Pd alloy catalysts which are associated with the enhancement in activity we observe for the bi-metallic catalysts.

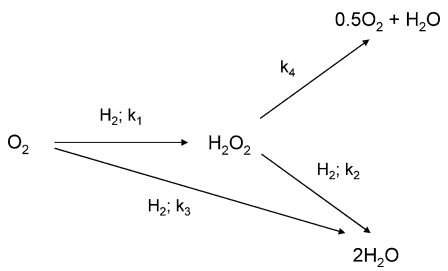

Scheme 2

Table 2 Effect of Br^- and H_3PO_4 on hydrogen peroxide synthesis[107]

Catalyst	Productivity[a]
2.5 wt% Au–2.5 wt% Pd/TiO_2	64
2.5 wt% Au–2.5 wt% Pd/TiO_2	53[b]
2.5 wt% Au–2.5 wt% Pd/TiO_2	4[c]
2.5 wt% Au–2.5 wt% Pd/carbon	110
2.5 wt% Au–2.5 wt% Pd/carbon	20[c]
5 wt% Pd/$BaSO_4$	21
5 wt% Pd/$BaSO_4$	80[c]
5 wt% Pd/Carbon	15
5 wt% Pd/Carbon	110[c]

[a] Standard conditions with CO_2 as diluent: 420 psi 5% H_2/CO_2 + 150 psi 25% O_2/CO_2, 4 vol% H_2, 2 °C, solvent (5.6 g MeOH and 2.9 g H_2O), H_2 : O_2 molar ratio = 1 : 2, 3.7 MPa, stirring at 1200 rpm, catalyst 10 mg. [b] Standard reaction conditions with H_3PO_4 (1.6 M), 0.0006 M NaBr. [c] Reaction carried out according to Van Weynbergh *et al.*[114]: H_3PO_4 (30 ml, 1.6 M), NaBr (0.0006 M), catalyst 30 mg, 25 °C, 420 psi 5% H_2/CO_2 + 150 psi 25% O_2/CO_2, stirring at 1200 rpm.

We have used CO_2 as a diluent since this diluent provides the smallest explosive region for H_2/O_2 mixtures. Our choice proved to be fortuitous,[107] as CO_2 has a marked effect on the reaction, since in the absence of CO_2 much lower yields of hydrogen peroxide are obtained (Table 3). CO_2 is soluble in the solvent and the degree of solubility is favoured by the low reaction temperature (2 °C) and high partial pressure of CO_2 (3.1 MPa). The carbonic acid that is formed acts as an *in situ* acidic promoter stabilising the hydrogen peroxide that is formed. We calculated that the pH of the solvent during the reaction using CO_2 as diluent will be *ca.* 4. When using N_2 as diluent, in place of CO_2, with a solvent acidified with HNO_3 to pH 4, we obtained an enhancement in the yield of hydrogen peroxide that is directly comparable to that observed when CO_2 is present. However, CO_2 has the advantage that the effect is reversible since upon depressurisation the CO_2 is degassed from the hydrogen peroxide solution and hence it operates as a reversible *in situ* promoter. This effect of *in situ* acid generation using CO_2 in the direct hydrogen peroxide synthesis has also been observed in previous studies by Hâncu and Beckman,[115] and we consider that the use of CO_2 could be highly beneficial in the direct hydrogen peroxide synthesis reaction.

Table 3 Effect of CO_2 diluent on the synthesis of hydrogen peroxide.[107]

Catalyst	Productivity
2.5 wt% Au–2.5 wt% Pd/TiO_2	64[a]
2.5 wt% Au–2.5 wt% Pd/TiO_2	29[b]
2.5 wt% Au–2.5 wt% Pd/G60	110[a]
2.5 wt% Au–2.5 wt% Pd/G60	10[b]

[a] Standard conditions with CO_2 as the diluent: 420 psi 5% H_2/CO_2 + 150 25% O_2/CO_2, 4 vol% H_2, 2 °C, solvent (5.6 g MeOH and 2.9 g H_2O), H_2 : O_2 molar ratio = 1 : 2, 3.7 MPa, stirring at 1200 rpm. [b] N_2 used as the diluent: 5% H_2/Ar (290 psig) + 10% O_2/He (290 psig), 4 vol% H_2, 2 °C, solvent (5.6 g MeOH and 2.9 g H_2O), H_2 : O_2 molar ratio = 1 : 2, 3.7 MPa, stirring at 1200 rpm.

We have investigated the structure of the active Au–Pd catalysts in detail, particularly using transmission electron microscopy.[105,109] It is essential that the catalysts are calcined at 400 °C as otherwise gold and palladium leach from the catalyst under the reaction conditions and the catalysts cannot be reused. This is unfortunate as the uncalcined materials are particularly active and selective for hydrogen peroxide synthesis. We have observed that the calcined catalysts are all alloys but that the oxide-supported Au–Pd materials comprise core shell structures with a Pd-rich shell and a Au-rich core. Clearly the Au must be modifying the structure of the surface layer of the alloy nanoparticles as otherwise only the catalytic performance of Pd would be observed for these catalysts, and this is clearly not the case. The core shell structure develops during the calcination procedure[103] and the Pd-rich shell becomes more pronounced at higher temperatures (Fig. 14). In addition, during the calcination non-alloyed metals present in the fresh uncalcined materials become alloyed and this plays a role in stabilising the metals under reaction conditions. However, the core–shell structures do not appear, at this stage, to be important in the observed catalysis, and we consider that they are a consequence of the sintering process on an oxide support. The Pd becomes oxidised to Pd^{2+} and this preferentially is stabilised on the surface of the nanoparticles. The reason why we consider the core–shell structures to be less important at this time, is that the most active catalysts are formed on carbon supports, and these form homogeneous alloys.[105] The key observation is that the carbon support stabilises a much smaller particle size distribution of the Au–Pd nanoparticles when compared with the TiO_2-supported catalyst.[105] However, it is apparent that the method of preparation used to generate the materials, which is based on wet impregnation, produces a very broad particle size distribution even on the carbon support (Fig. 15). As stated previously these broad particle size distributions have their value at the catalyst discovery stage of an investigation, since one maximises the chances of observing activity. It is known that the Au and Pd concentrations vary markedly with particle size.[108] The smallest particles contain almost exclusively Pd and the concentration of Au increases as the particle size increases, consequently with this method of preparation both the particle size and composition can be explored. We currently consider that it is the small 2–3 nm particles that are responsible for the enhanced activity. We have, very recently, used a sol-immobilisation preparation procedure[106] that gives a very narrow particle size distribution of small alloy nanoparticles, and have shown that this leads to enhanced activity. The key aspect of future studies will be to identify improved preparation methods to ensure that a high concentration of the small nanoparticles is both achieved and maintained.

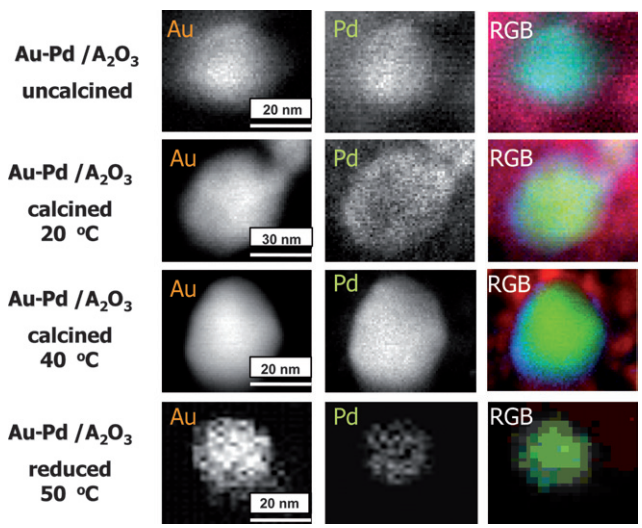

Fig. 14 A montage of (a) Au L_α XEDS map (b) Pd L_α XEDS map and (c) RGB overlays (green: Au, blue: Pd) for a series of $AuPd/Al_2O_3$ samples subjected to different thermal treatments. *Row 1*: dried at 120 °C. *Row 2*: calcined at 200 °C. *Row 3*: calcined at 400 °C. *Row 4*: calcined at 400 °C then reduced at 500 °C in H_2.[108]

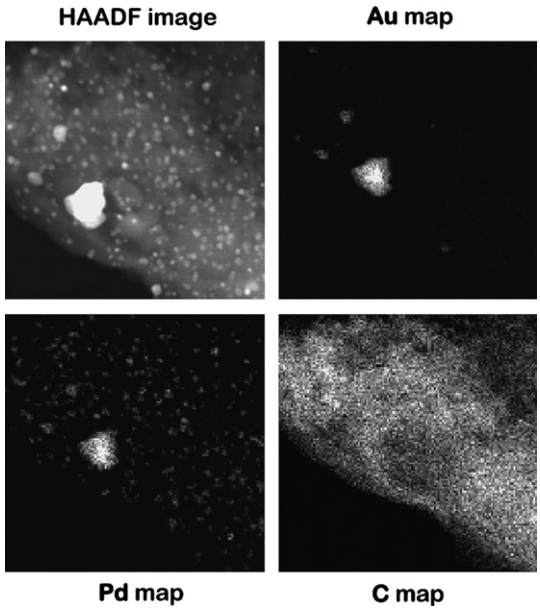

Fig. 15 HAADF STEM image and Au, Pd and C STEM XEDS maps showing the spatial and chemical distribution of alloy particles in the uncalcined 2.5 wt% Au–2.5 wt% Pd/carbon.[105]

Concluding remarks and future perspectives

As noted in the introduction, the three catalysts chosen for detailed discussion in this feature paper were selected to demonstrate some of the complex structural features that are encountered in real catalysts. Unfortunately, it is apparent that there is no unifying methodology that can be used to design catalysts *a priori* using current methodologies. However, the two related methods described, using the virtual mechanistic approach, do indicate that these methods can be used to identify initial catalyst compositions that should be evaluated in detail. To date, however, very limited use of this methodology has been reported. However, there is an increasing use of theoretical studies as an aid to understanding how and why catalysts function, and it is possible that such mechanistic approaches can be beneficial in designing novel, more efficient catalysts.

The identification of new heterogeneous catalysts has two distinct phases. The initial phase is catalyst discovery, which is where we need to address new approaches. The subsequent stage of catalyst design involves optimisation of the initial

formulations. Catalyst discovery can be aided by the most up to date high through-put preparation and testing techniques, as well as theoretical studies, and this is where the application of materials science methodology could be of great benefit. For example, it is quite likely that both the supported gold catalysts and the vanadium phosphate catalysts could have been discovered using high through-put methods. Of course the detailed follow up studies would have been needed to uncover the complexities of these catalysts and gain an understanding of the nature of the active sites. In addition, it is clear that as gold catalysis advances we will need more sophisticated methods to produce nanoparticles of the required small sizes with specific compositions. Another important feature that has to be considered is the stability of the active catalytic structures. Often the catalyst lifetime associated with new catalyst discoveries can be quite short and detailed studies are required to ensure stable structures and catalytic performance can be achieved. Again, this is an area where a materials science approach can be expected to make significant progress in the design of improved heterogeneous catalysts. At present, there are relatively few studies that make this connection, but it is clear that significant advances can be expected if this connection is achieved.

References

1 M. Taramasso, G. Perego, and B. Notari, *US Pat.*, 4 410 501, 1983.
2 A. Corma, *Chem. Rev.*, 1997, **97**, 2373.
3 A. Corma, *Chem. Rev.*, 1995, **95**, 559.
4 A. Corma, *J. Catal.*, 2003, **216**, 298.
5 A. Corma, M. Diaz-Cabanas, J. Martinez-Triguero, F. Rey and J. Ruis, *Nature*, 2002, **418**, 514.
6 C. T. Kresge, M. E. Leonowitz, W. J. Roth, J. C. Vartoli and J. S. Beck, *Nature*, 1992, **359**, 710.
7 A. S. Kharitonov, T. N. Alexandrova, L. A. Vostrikova, K. G. Ione and G. I. Panov, *Russ. Pat.* 4 445 646, 1988.
8 M. Haruta, T. Kobayashi, H. Sano and N. Yamada, *Chem. Lett.*, 1987, **16**, 405.
9 A. Corma, S. Iborra and A. Velby, *Chem. Rev.*, 2007, **107**, 2411.
10 C. Perego, A. Carati, P. Ingallina, M. Mantegazza and G. Bellussi, *Appl. Catal. A*, 2001, **221**, 63.
11 A. K. Sinha, S. Seelan, S. Tsubota and M. Haruta, *Angew. Chem., Int. Ed.*, 2004, **43**, 1546.
12 R. A. Sheldon, M. Wallau, I. W. C. E. Arends and U. Schuchardt, *Acc. Chem. Res.*, 1998, **31**, 485.
13 L. Davies, P. McMorn, D. Bethell, P. C. Bulman Page, F. King, F. E. Hancock and G. J. Hutchings, *Chem. Commun.*, 2000, 1807.
14 T. Ito and J. H. Lunsford, *Nature*, 1985, **314**, 721.
15 G. J. Hutchings, M. S. Scurrell and J. R. Woodhouse, *J. Chem. Soc., Chem. Commun.*, 1988, 253.
16 D. A. Dowden and G. T. Walker, *UK Pat.* 1 244 001, 1971.
17 J. S. J. Hargreaves, G. J. Hutchings, R. W. Joyner and S. H. Taylor, *Chem. Commun.*, 1996, 523.
18 D. Wolf, O. V. Buyevskaya and M. Baerns, *Appl. Catal., A*, 2000, **200**, 63.
19 R. L. Bergman and N. W. Frisch, *US Pat.*, 3 293 268, 1966.
20 G. Centi, *Catal. Today*, 1994, 16.
21 E. Bordes, *Catal. Today*, 1987, **1**, 499.
22 J. T. Gleaves, J. R. Ebner and T. C. Knechler, *Catal. Rev. Sci. Eng.*, 1988, **30**, 49.
23 G. Centi, F. Trifirò, G. Busca, J. Ebner and J. Gleaves, *Faraday Discuss.*, 1989, **87**, 215.
24 G. J. Hutchings, *J. Mater. Chem.*, 2004, **14**, 3385.
25 C. J. Kiely, A. Burrows, S. Sajip, G. J. Hutchings, M. T. Sananes, A. Tuel and J. C. Volta, *J. Catal.*, 1996, **162**, 31.
26 C. J. Kiely, A. Burrows, G. J. Hutchings, K. E. Bere, J. C. Volta, A. Tuel and M. Abon, *J. Chem. Soc., Faraday Disc.*, 1996, **105**, 103.
27 J. A. Lopez-Sanchez, L. Griesel, J. K. Bartley, R. P. K. Wells, A. Liskowski, D. Su, R. Schlögl, J.-C. Volta and G. J. Hutchings, *Phys. Chem. Chem. Phys.*, 2003, **5**, 3525.
28 W. S. Dong, J. K. Bartley, N. F. Dummer, F. Girgsdies, D. Su, R. Schlögl, J. C. Volta and G. J. Hutchings, *J. Mater. Chem*, 2005, **15**, 3214.
29 N. Hiyoshi, N. Yamamoto, N. Ryamon, Y. Kamiya and T. Ohuhara, *J. Catal.*, 2004, **221**, 225.
30 H. Imai, Y. Kamiya and T. Okuhara, *J. Catal.*, 2007, **251**, 195.
31 G. J. Hutchings, J. A. Lopez-Sanchez, J. K. Bartley, J. M. Webster, A. Burrows, C. J. Kiely, A. F. Carley, C. Rhodes, M. Hävecker, A. Knop-Gericke, R. W. Mayer, R. Schlögl, J. C. Volta and M. Poliakoff, *J. Catal.*, 2002, **208**, 197.
32 V. V. Guliants, J. B. Benziger, S. Sundaresan, I. E. Wachs, J.-M. Jehng and J. E. Roberts, *Catal. Today*, 1996, **28**, 275.
33 V. V. Guliants, J. B. Benziger, S. Sundaresan, N. Yao and I. E. Wachs, *Catal. Lett.*, 1995, **32**, 3.
34 G. J. Hutchings, A. Desmartin Chomel, R. Olier and J. C. Volta, *Nature*, 1994, **368**, 41.
35 M. R. Thompson, A. C. Hess, J. B. Nicholas, J. C. White, J. Anchell and J. R. Ebner, *Stud. Surf. Sci. Catal*, 1994, **82**, 167.
36 H. Berndt, K. Buker, A. Martin, A. Bruckner and B. Lucke, *J. Chem. Soc., Faraday Trans.*, 1995, **91**, 725.
37 S. Albonetti, F. Cavani, F. Trifiro, P. Venturoli, G. Calestani, M. L. Granados and J. L. G. Fierro, *J. Catal.*, 1996, **160**, 52.
38 S. Zeyss, G. Wendt, K. H. Hallmeier, R. Szargan and G. Lippold, *J. Chem. Soc., Faraday Trans.*, 1996, **92**, 3273.
39 A. Bruckner, A. Martin, N. Steinfeldt, G. U. Wold and B. Lucke, *J. Chem. Soc., Faraday Trans.*, 1996, **92**, 4257.
40 A. Bruckner, B. Kubias and B. Lucke, *Catal. Today*, 1996, **32**, 215.
41 W. H. Cheng and W. Wang, *Appl. Catal., A*, 1997, **156**, 57.
42 F. Meunier, P. Delporte, B. Heinrich, C. Bouchy, C. Crouzet, C. Phamhuu, P. Panissod, J. L. Leroud, P. L. Mills and M. J. Ledoux, *J. Catal.*, 1997, **169**, 33.
43 K. Aitlachgar, A. Tuel, M. Brun, J. M. Herrmann, J. M. Krafft, J. R. Martin, J. C. Volta and M. Abon, *J. Catal.*, 1998, **177**, 224.
44 A. Bruckner, A. Martin, B. Kubias and B. Lucke, *J. Chem. Soc., Faraday Trans.*, 1998, **94**, 2221.
45 A. Martin, G. U. Wolf, U. Steinike and B. Lucke, *J. Chem. Soc., Faraday Trans.*, 1998, **94**, 2227.
46 P. Delichere, K. E. Bere and M. Abon, *Appl. Catal., A*, 1998, **172**, 295.
47 M. Ruitenbeck, A. J. van Dillen, A. Barbon, E. E. van Faassen, D. C. Koningsberger and J. W. Geus, *Catal. Lett.*, 1998, **55**, 133.
48 P. Ruiz, Ph. Bastians, L. Caussin, R. Reuse, L. Daza, D. Acosta and B. Delmon, *Catal. Today*, 1993, **16**, 99.
49 H. Morishige, J. Tamaki, N. Msura and N. Yamazoe, *Chem. Lett.*, 1990, 1513.
50 S. Sajip, C. Rhodes, J. K. Bartley, A. Burrows, C. J. Kiely and G. J. Hutchings, in *Catalytic Activation and Functionalisation of Light Alkanes*, ed. E. G. Derouane, Kluwer, Dordrecht, 1998, p. 429.
51 V. V. Guliants, S. A. Holmes, J. B. Benziger, P. Heaney, D. Yates and I. E. Wachs, *J. Mol. Catal. A*, 2001, **172**, 265.
52 G. J. Hutchings, *Appl. Catal.*, 1991, **72**, 1.
53 G. J. Hutchings and R. Higgins, *J. Catal.*, 1996, **162**, 153.
54 S. Sajip, J. K. Bartley, A. Burrows, M.-T. Sananes Schulz, A. Tuel, J. C. Volta, C. J. Kiely and G. J. Hutchings, *New J. Chem.*, 2001, **25**, 125.
55 G. J. Hutchings, J. K. Bartley, J. M. Webster, J. A. Lopez-Sanchez, D. J. Gilbert, C. J. Kiely, A. F. Carley, S. M. Howdle, S. Sajip, S. Caldarelli, C. Rhodes, J. C. Volta and M. Poliakoff, *J. Catal.*, 2001, **197**, 232.
56 D. J. Dixon, G. Luna-Bercenas and K. P. Johnston, *Polymer*, 1994, **35**, 3998.
57 A. O'Neil, C. Wilson, J. M. Webster, F. J. Allison, J. A. K. Howard and M. Poliakoff, *Angew. Chem., Int. Ed.*, 2002, **41**, 3796.
58 C. N. Field, P. A. Hamley, J. M. Webster, D. H. Gregory, J. J. Titman and M. Poliakoff, *J. Am. Chem. Soc.*, 2000, **122**, 2480.
59 E. Reverchon, G. Della Porta, D. Sannino and P. Ciambelli, *Powder Technol.*, 1999, **102**, 127.
60 Z.-R. Tang, J. K. Edwards, J. K. Bartley, S. H. Taylor, A. F. Carley, A. A. Herzing, C. J. Kiely and G. J. Hutchings, *J. Catal.*, 2007, **249**, 208.
61 M. Conte, G. Budroni, J. K. Bartley, S. H. Taylor, A. F. Carley, A. Schmidt, D. M. Murphy, F. Girgsdies, T. Ressler, R. Schlögl and G. J. Hutchings, *Science*, 2006, **313**, 1270.

62 A. S. K. Hashmi, *Gold Bull*, 2004, **37**, 51.
63 G. C. Bond and D. T. Thompson, *Catal. Rev. Sci. Eng.*, 1999, **41**, 319.
64 G. C. Bond and D. T. Thompson, *Gold Bull.*, 2000, **33**, 41.
65 M. Haruta, *Gold Bull.*, 2004, **37**, 27.
66 R. Meyer, C. Lemaire, Sh. K. Shaikutdinov and H.-J. Freund, *Gold Bull.*, 2004, **37**, 72.
67 G. J. Hutchings, *Gold Bull.*, 2004, **37**, 37.
68 A. S. K. Hashmi and G. J. Hutchings, *Angew. Chem., Int. Ed.*, 2006, **45**, 7896.
69 M. Haruta, *CATTECH*, 2002, **6**, 102.
70 D. T. Thompson, *Appl. Catal. A*, 2003, **243**, 201.
71 G. J. Hutchings, *Catal. Today*, 2005, **100**, 55.
72 G. J. Hutchings and M. Haruta, *Appl. Catal., A*, 2005, **291**, 2.
73 G. J. Hutchings, *Chem. Comm.*, 2008, 1148.
74 M. Haruta, *Nature*, 2005, **437**, 1098.
75 G. J. Hutchings, *J. Catal.*, 1985, **96**, 292.
76 M. Haruta, N. Yamada, T. Kobayashi and S. Iijima, *J. Catal. 1989*, **115**, 301.
77 G. J. Hutchings, *Dalton Trans.*, 2008, 5523.
78 M. Haruta, H. Kageyama, N. Kamijo, T. Kobayashi and F. Delannay, *Stud. Surf. Sci. Catal.*, 1989, **44**, 33.
79 F. Moreau, G. C. Bond and A. O. Taylor, *J. Catal.*, 2005, **231**, 105.
80 R. Zanella, S. Giorgio, C. R. Henry and C. Louis, *J. Phys. Chem. B*, 2002, **106**, 7634.
81 R. Zanella, L. Delannoy and C. Louis, *Appl. Catal., A*, 2005, **291**, 62.
82 R. Zanella and C. Louis, *Catal. Today*, 2005, **107–108**, 768.
83 N. A. Hodge, C. J. Kiely, R. Whyman, M. R. H. Siddiqui, G. J. Hutchings, Q. A. Pankhurst, F. E. Wagern, R. R. Rajaram and S. E. Golunski, *Catal. Today*, 2002, **72**, 133.
84 P. Landon, J. Ferguson, B. E. Solsona, T. Garcia, A. F. Carley, A. A. Herzing, C. J. Kiely, S. E. Golunski and G. J. Hutchings, *Chem. Commun.*, 2005, 3385.
85 P. Landon, J. Ferguson, B. E. Solsona, T. Garcia, S. Al-Sayari, A. F. Carley, A. A. Herzing, C. J. Kiely, M. Makkee, J. A. Moulijn, A. Overweg, S. E. Golunski and G. J. Hutchings, *J. Mater. Chem*, 2006, **16**, 199.
86 S. N. Rashkeev, A. R. Lupini, S. H. Overbury, S. J. Pennycook and S. T. Pantelides, *Phys. Rev. B*, 2007, **76**, 35438.
87 G. J. Hutchings, M. S. Hall, A. F. Carley, P. Landon, B. E. Solsona, C. J. Kiely, A. Herzing, M. Mckee, J. A. Moulijn, A. Overweg, J. C. Fierro-Gonzalez, J. Guzman and B. C. Gates, *J. Catal.*, 2006, **242**, 71.
88 A. A. Herzing, C. J. Kiely, A. F. Carley, P. Landon and G. J. Hutchings, *Science*, 2008, **321**, 1331.
89 M. S. Chen and D. W. Goodman, *Science*, 2004, **306**, 252.
90 A. Abad, P. Concepion, A. Corma and H. Garcia, *Angew. Chem., Int. Ed.*, 2005, **44**, 4066.
91 A. K. Sinha, S. Seelan, S. Tsubota and M. Haruta, *Angew. Chem., Int. Ed.*, 2004, **43**, 1546.
92 M. D. Hughes, Y.-J. Xu, P. Jenkins, P. McMorn, P. Landon, D. I. Enache, A. F. Carley, G. A. Attard, G. J. Hutchings, F. King, E. H. Stitt, P. Johnston, K. Griffin and C. J. Kiely, *Nature*, 2005, **437**, 1132.
93 J. M. Campelo, T. D. Conesa, M. J. Gracia, M. J. Jurado, R. Luque, J. M. Marinas and A. A. Romero, *Green Chem.*, 2008, **10**, 853.
94 P. Lignier, E. Morfin, S. Mangematin, L. Massin, J. L. Roust and V. Caps, *Chem. Commun.*, 2007, 168.
95 M. Turner, V. B. Golovko, O. P. H. Vaughan, P. Abdulkin, A. Berenguer-Murcia, M. S. Tikhov, B. F. G. Johnson and R. M. Lambert, *Nature*, 2008, **454**, 981.
96 J. E. Bailie and G. J. Hutchings, *Chem. Commun.*, 1999, 2151.
97 Y. Segura, N. López and J. P. Ramírez, *J. Catal.*, 2007, **247**, 383.
98 A. Corma, C. Gonzalez-Arellano, M. Iglesias and F. Sanchez, *Angew. Chem., Int. Ed.*, 2007, **46**, 7820.
99 A. Corma and P. Serna, *Science*, 2006, **313**, 332.
100 P. Landon, P. J. Collier, A. J. Papworth, C. J. Kiely and G. J. Hutchings, *Chem. Commun.*, 2002, 2058.
101 P. Landon, P. J. Collier, A. F. Carley, D. Chadwick, A. J. Papworth, A. Burrows, C. J. Kiely and G. J. Hutchings, *Phys. Chem. Chem. Phys.*, 2003, **5**, 1917.
102 B. E. Solsona, J. K. Edwards, P. Landon, A. F. Carley, A. Herzing, C. J. Kiely and G. J. Hutchings, *Chem. Mater.*, 2006, **18**, 2689.
103 J. K. Edwards, B. Solsona, P. Landon, A. F. Carley, A. Herzing, M. Watanabe, C. J. Kiely and G. J. Hutchings, *J. Mater. Chem.*, 2005, **15**, 4595.
104 J. K. Edwards, B. Solsona, P. Landon, A. F. Carley, A. Herzing, C. J. Kiely and G. J. Hutchings, *J. Catal.*, 2005, **236**, 69.
105 J. K. Edwards, A. F. Carley, A. A. Herzing, C. J. Kiely and Graham J. Hutchings, *J. Chem. Soc., Faraday Disc.*, 2008, **138**, 225.
106 J. A. Lopez-Sanchez, N. Dimitratos, P. Miedziak, E. Ntainjua, J. K. Edwards, D. Morgan, A. F. Carley, R. Tiruvalam, C. J. Kiely and G. J. Hutchings, *Phys. Chem. Chem. Phys*, 2008, **10**, 1921.
107 J. K. Edwards, A. Thomas, A. F. Carley, A. A. Herzing, C. J. Kiely and G. J. Hutchings, *Green Chem.*, 2008, **10**, 388.
108 A. A. Herzing, M. Watanabe, J. K. Edwards, M. Conte, Z. R. Tang, G. J. Hutchings and C. J. Kiely, *J. Chem. Soc., Faraday Disc.*, 2008, **138**, 337.
109 D. I. Enache, J. K. Edwards, P. Landon, B. Solsona-Espriu, A. F. Carley, A. A. Herzing, M. Watanabe, C. J. Kiely, D. W. Knight and G. J. Hutchings, *Science*, 2006, **311**, 362.
110 H. T. Hess, in *Kirk-Othmer Encyclopaedia of Chemical Engineering*, ed. I. Kroschwitz and M. Howe-Grant, Wiley, New York, 1995, vol. 13, p. 961.
111 V. R. Choudhary and C. Samanta, *J. Catal.*, 2006, **238**, 28.
112 C. Samanta and V. R. Choudhary, *Catal. Commun.*, 2006, **8**, 73.
113 V. R. Choudhary, C. Samanta and P. Jana, *Appl. Catal., A*, 2007, **317**, 234.
114 J. van Weynbergh, J.-P. Schoebrechts and J.-C. Colery, *US Pat.*, 5 447 706, 1995.
115 D. Hâncu and E. J. Beckman, *Green Chem.*, 2001, **3**, 8.